Research Square

Preprints are preliminary reports that have not undergone peer review.
They should not be considered conclusive, used to inform clinical practice,
or referenced by the media as validated information.

Continuous-flow magnesium electrocoagulation for nutrient recovery from Phosphate- limited domestic wastewater: effects of pH and applied current

Yulisya Zuriatni
Institut Teknologi PLN
Gani Purwiandono
gani_purwiandono@uii.ac.id
Universitas Islam Indonesia
Rachmad Ardhianto
Institut Teknologi PLN
Nurcahyo Iman Prakoso
Universitas Islam Indonesia
Tatang Shabur Julianto
Universitas Islam Indonesia

Research Article

Keywords: magnesium electrocoagulation, continuous-flow, ammonium removal, phosphate removal, struvite recovery, energy consumption

Posted Date: November 26th, 2026

DOI: https://doi.org/10.21203/rs.3.rs-11715713/v1

License: This work is licensed under a Creative Commons Attribution 4.0 International License.
Read Full License

Additional Declarations: No competing interests reported.

Continuous-flow magnesium electrocoagulation for nutrient recovery from Phosphate-limited domestic wastewater: effects of pH and applied current

Yulisya Zuriatni[1,2], Gani Purwiandono[1,*], Rachmad Ardhianto[3], Nurcahyo Iman Prakoso[1], and Tatang Shabur Julianto[1]

[1]Department of Chemistry, Faculty of Mathematics and Natural Sciences, Universitas Islam Indonesia, Yogyakarta 55584, Indonesia
[2]Department of Civil Engineering, Faculty of Regional and Infrastructure Technology, Institut Teknologi PLN, Jakarta 11480, Indonesia
[3]Department of Environmental Engineering, Faculty of Regional and Infrastructure Technology, Institut Teknologi PLN, Jakarta 11480, Indonesia

Corresponding author: gani_purwiandono@uii.ac.id

Abstract

The capability of continuous-flow magnesium electrocoagulation (EC-Mg) to simultaneously eliminate nutrients and potentially recover struvite from phosphate-limited domestic wastewater under different pH conditions and applied currents was investigated. The effects of pH levels between 7 and 9 and currents of 3, 5, and 10 A on the removal of phosphate and ammonium, reduction of total suspended solids (TSS), energy consumption, and precipitate characteristics were assessed. Phosphate removal was significantly affected by pH, with an optimal removal of 91.27 ± 4.15% at pH 8 and 5. In contrast, ammonium removal exhibited a different pattern, with the highest removal rate of 71.46% at pH 9 and 5–10 A, suggesting that ammonium removal was less sensitive to pH than phosphate removal was. Increasing the current from 3 to 5 A enhanced magnesium dissolution and nutrient removal; however, further increasing it to 10 A resulted in excessive energy use without improving nutrient removal. The TSS removal was approximately 96% at pH 8–10. Overall, pH 8 and 5 A were the most balanced operating conditions for continuous EC-Mg, offering effective nutrient removal, and reduced energy demand while maintaining the potential for nutrient recovery.

Keywords: magnesium electrocoagulation; continuous-flow; ammonium removal; phosphate removal; struvite recovery; energy consumption

1. Introduction

Population growth, urbanisation, and changes in societal consumption patterns have increased the volume of domestic wastewater discharged annually. Domestic wastewater generally contains high concentrations of organic matter, suspended solids, nitrogen, and phosphorus, which can decrease the quality of water bodies if discharged without proper treatment [1] and [2]. Nitrogen and phosphorus are the main causes of eutrophication, which is characterised by excessive algal growth, decreased dissolved oxygen levels, and disruption of the aquatic ecosystem balance [3] and [4]. Therefore, wastewater treatment now focuses not only on meeting effluent quality standards but also on resource recovery as part of the circular economy concept and sustainable development [5] and [6].

One increasingly popular method for nutrient recovery is the formation of struvite ($MgNH_4PO_4 \cdot 6H_2O$), a phosphate mineral that can be used as a slow-release fertiliser. Struvite formation simultaneously removes ammonium and phosphate while producing value-added products. Theoretically, struvite crystallisation is influenced by the availability of magnesium ions (Mg^{2+}), ammonium (NH_4^+), phosphate (PO_4^{3-}), pH, and supersaturation conditions of the solution [7]. Therefore, many previous studies have added magnesium salts and adjusted the Mg:N:P molar ratio to approach the stoichiometric condition (1:1:1) to optimise the crystallisation process [8]. This method has been successfully applied to various types of wastewater, such as leachate, anaerobic digestate, urine, and livestock waste, with high phosphate content or that has been chemically adjusted [9].

However, the actual characteristics of domestic wastewater often do not match the ideal conditions used in previous studies. Domestic wastewater generally has a high ammonium content, whereas the phosphate concentration tends to be lower owing to consumption patterns, dilution, and prior treatment processes. This study identified that domestic wastewater exhibits an NH_4^+:PO_4^{3-} molar ratio of approximately 48:1, with phosphate being a limiting factor in struvite production. This indicates a significant nutrient imbalance relative to the theoretical ratio required for the synthesis of struvite. Nitrogen and phosphorus are concurrently recovered through chemical precipitation using $MgSO_4$ or electrocoagulation (EC) with Mg electrodes [10], [11]. Unlike conventional electrocoagulation methods that employ aluminum (Al) or iron (Fe) electrodes, which are ineffective in removing dissolved ammonium nitrogen, EC with Mg electrodes can directly eliminate both phosphorus and ammonium from wastewater. Based on Govindan et al [12]

reported that NH_3-N and PO_4^{3-} recovery rates can reach up to 90% within a pH range of 6–8 at a current density of 8 mA/cm², with a Mg^{2+}:NH_4^+ ratio of 1:1 and Mg^{2+}:PO_4^{3-} of 1.1:1. Furthermore, the efficacy of chemical precipitation (CP), batch electrocoagulation (BEC), and continuous electrocoagulation (CEC) in struvite ($MgNH_4PO_4 \cdot 6H_2O$) formation from synthetic wastewater was assessed. The results demonstrated phosphate reductions of 93.6%, 74.5%, and 71.6% for the BEC, CEC, and CP processes, respectively. Conversely, the ammonium reductions were 79.4%, 51.5%, and 62.5% for BEC, CEC, and CP, respectively [13].

The on-site generation of Mg^{2+} ions via electrical methods can promote their interaction with NH_4^+ and PO_4^{3-} ions, leading to the formation of struvite. This phosphate mineral, with the chemical formula $MgNH_4PO_4 \cdot 6H_2O$, serves as a source of essential nutrients for plants, including nitrogen, phosphorus, and magnesium. Struvite can replace synthetic fertilisers, thereby reducing their dependence on agricultural and plantation contexts. This substitution could also mitigate the risk of environmental pollution on both local and global scales [14], [15]. Compared with conventional chemical precipitation, electrocoagulation offers lower chemical requirements, a simpler process, and the potential to integrate nutrient recovery and pollutant removal processes within a single-unit operation. However, most electrocoagulation studies on struvite formation are still conducted in batch systems [16], and thus do not fully reflect the operational conditions of continuously operating wastewater treatment plants. Continuous electrocoagulation requires special attention to reactor design, electric current control, hydraulic retention time, and the prevention of phenomena such as electrode passivation, which can reduce the efficiency of nutrient recovery and struvite precipitation [17] and [18].

The approach to struvite recovery processes using a tubular reactor model was reported by [19] using a multi-rod helical system with a Mg anode that produced struvite compounds at $31.5 \pm 2.52\%$ struvite recovery in 25 min with a batch reactor. However, the potential of multi-rod helical system (MRHS) in continuous processes has been successfully employed on a large scale in previous studies in the electroplating and textile industries [20]–[21]. The continuous-flow magnesium tubular electrocoagulation reactor offers several advantages, including a more uniform electric field distribution, efficient mass transfer, continuous magnesium ion release, and ease of integration with large-scale wastewater treatment systems. However, research on the use of tubular electrocoagulation reactors with a continuous-flow MRHS system for struvite recovery from domestic wastewater with phosphate-limited characteristics remains limited. In addition, the

influence of key operating parameters, especially pH and current application, on struvite formation under the ratio conditions of NH_4^+:PO_4^{3-} which is very high, has not been widely reported. This study aimed to evaluate the performance of continuous-flow electrocoagulation in struvite recovery from domestic wastewater with phosphate-limited characteristics, based on the existing research gap. The effects of pH variation and current density on ammonium and phosphate removal efficiency, struvite crystal formation, and overall process performance were systematically analysed. The results of this study are expected to provide a scientific contribution to the development of continuous electrocoagulation technology for nutrient recovery from domestic wastewater with extreme nutrient imbalance, as well as support the application of the circular economy concept through the reutilisation of nitrogen and phosphorus as valuable resources.

2. Methods and Results

2.1.Characteristics of fed wastewater

The wastewater used in this study was sourced from academic activities at the ITPLN campus in Duri Kosambi, West Jakarta, Indonesia. It predominantly originates from urination rather than from defaecation. Wastewater was pumped from a collection tank before the treatment. The BOD/COD ratio indicates that the wastewater contains a considerable amount of dissolved organic matter, although its value is lower at 0.3 when compared to the average domestic wastewater, which generally reaches values in the hundreds to thousands. The pH value of 8.17 ±0.20 is shown in Table 1. A TSS value of 116.00 mg/L indicates a moderate amount of settleable suspended solids. According to [22], the average TSS value of Indonesian domestic wastewater is approximately 1986.8 mg/L. This TSS level can affect both the electrocoagulation and crystallisation processes because the suspended particles can act either as diffusion barriers or as nucleation sites for crystal formation. An increase in TSS not only results in decreased struvite recovery but also reduces struvite purity. Subsequently, a molar ratio analysis was conducted to evaluate the feasibility of struvite formation based on the balance of nitrogen and phosphorus with respect to the theoretical stoichiometry of Mg:N:P = 1:1:1. The ammonium and phosphorus concentrations were 42.24 mg/L and 4.623 mg/L, respectively, yielding an N:P molar ratio of 48:1. These results indicate that nitrogen acts as an excess reactant and phosphorus as a limiting reactant. In addition, high ammonium concentrations can increase the recovery and purity of struvite [23].

Table 1. Characteristics of the fed wastewater

No	Parameters	Value	Unit
1	pH	8.17 ±0.20	-
2	Biochemical oxygen demand (BOD)	96.33 ±34.07	mg/L
3	Chemical Oxygen Demand	320.50 ± 113.64	mg/L
4	Total suspended solids (TSS)	116.00 ± 25.51	mg/L
5	Ammonia, NH_3-N	54.59 ± 48.69	mg/L
6	Ammonium (NH_4^+)	42.242 ± 3.47	mg/L
7	Phospate (PO_4^{3-})	4.623 ± 1.08	mg/L
8	BOD/COD	0.3	-
9	N:P	48:1	-

2.2.Reactor configuration

The study used an electrocoagulation (EC) reactor, which is a tubular device that operates continuously with an Mg anode and MRHS serving as the cathode, as shown in Figure 1. The reactor included a wastewater holding tank measuring 300 mm × 300 mm × 550 mm in size. The reaction chamber unit of the EC process comprised two reactors, each with a diameter of 50 mm and a height of 532 mm.

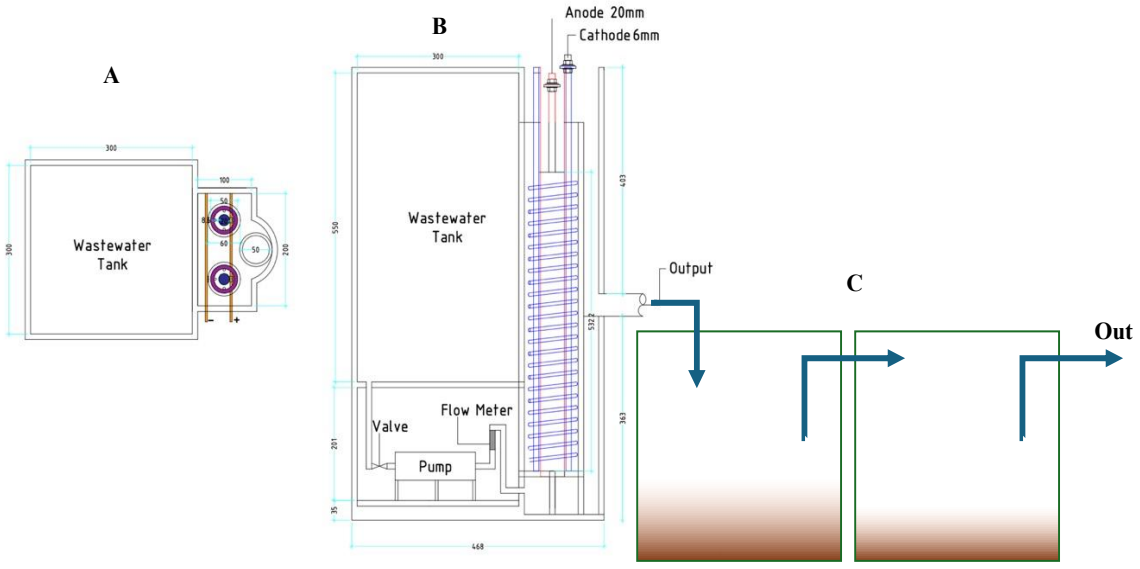


Figure 1. Configuration of electrocoagulation in a tubular system using a Mg anode (A. Top view of the reactor, B. reactor section, and C. sedimentation tank)

As shown in Figure 1, the cathode system featured an MRHS configure ration with an outer diameter of 480 mm, constructed from stainless steel 201 with a thickness of 6 mm, and included two units. The Mg anode consisted of two units, each with dimensions of 20 mm in diameter and 500 mm in length, made from Mg alloy extruded rods (Liaofu, China). A pump with a capacity of 1–4 Lpm facilitated water circulation through an upflow system, supporting the EC system. The EC system (CEC) was linked to a DC switching power supply (Haney-6030A) delivering 60 V and 30 A, supplied by Haney Electrochemical Ltd., China. Figure 1 depicts the top view of the EC reactor, and Figure 1B details the reactor components. Image C in Figure 1 illustrates the settling chamber, with each holding tank measuring 250 mm × 250 mm × 400 mm in size. Following the EC process, the output was transferred to a precipitation process using a sedimentation tank with a total volume of 50 L divided into two 25 L tanks. The sedimentation supernatant was analysed for ammonium and phosphate levels, and the resulting sludge was collected for further analysis.

2.3.Measurement methods

In accordance with the Standard Methods for the Examination of Water and Wastewater, assessments were conducted for TDS, TSS, ammonium, phosphate, ORP, and pH. TSS was determined using a gravimetric approach, whereas pH, TDS, and ORP were assessed using the digital devices Lutron PH 201, YK-22CTA, and WA-2017SD, respectively. Ammonium and phosphate were quantified using spectrophotometry (Hach DR 3900, USA) at 640 and 680 nm, respectively.

2.4.Analysis of precipitates

Following each batch experiment, approximately 0.45 mm precipitated particles were obtained by filtration. The samples were analysed for ammonium and phosphate. The X-ray diffraction (XRD) was used to examine the precipitate from one experiment and the anode surface films from two tests using a Bruker D2 instrument. Data evaluation was conducted using Match! 2 software (Match! Crystal Impact, Bonn, Germany). The sludge surfaces were examined by scanning electron microscopy (SEM) equipped with energy-dispersive X-ray spectroscopy (EDX) using a Fourier-emission scanning electron microscope (FESEM) Thermo Scientific Quattro S instrument at the Mining Technology Research Center of BRIN (South Lampung). To lower and raise the pH, 32% HCl solution and 48% NaOH (w/w) were supplied by PT Selaras Alam Varia Energy, Bandung, West Java, Indonesia.

2.5.Data collection and analysis

The elimination efficiencies of ammonium, phosphate, and TSS in the EC anode using Mg were calculated using equation 1.

$$R\ (\%) = \frac{C_t - C_0}{Co} x\ 100\% \quad (1)$$

where R represents the removal efficiency, C_0 is the initial concentration of the feed solution (mg/L), and C_t is the concentration of ammonium, phosphate, and TSS in the concentrated compartment (mg/L). The amount of metal ions dissolved in the EC was calculated using Faraday's law (equation 2) (Cherifi et al., 2016; Singh & Ramesh, 2014).

$$m_{theoretical} = \frac{I\ x\ t\ x\ M}{z\ x\ F\ x\ V} \quad (2)$$

According to equation 3, the current density of the anode during continuous EO processes varied depending on the supplied current and the change in the anode surface area.

$$j = \frac{I}{A} \quad (3)$$

where j is the current density (A/m^2), I the applied current (A), and A the electrode surface area (m^2). The major component of EC is energy consumption [26], which can be calculated using equation 4.

$$C_{energy} = \frac{U\ x\ i\ x\ t}{V} \quad (4)$$

where C_{energy} is the energy consumption (kWh/m^3), U is the applied voltage (V), i is the applied current (A), t is the EC time (h), and V is the wastewater volume (m^3).

2.6.Experimental Design

In this study, the independent variables were the pH of the wastewater (7, 8, and 9) and the applied current (3, 5, and 10 A). The selection of pH as an independent variable was based on its crucial role in determining the effectiveness of the ammonium removal. Samples were collected at 0, 5, 10, 20, 30, 40, 50, and 60 min after settling. The effects of the independent variables on the concentration and removal efficiency of ammonium, phosphate, and TSS after the process were analysed using Minitab 21. Normality and homogeneity of the data were assessed before hypothesis testing. The Shapiro–Wilk test was used to examine residual normality, and Levene's test was employed to assess variance homogeneity [27]. If the data were normally distributed and homogeneous, a parametric hypothesis test (ANOVA) was applied, followed by a post hoc Tukey's HSD test for further data analysis [28]. However, if either assumption was not met, a

nonparametric hypothesis test (Kruskal–Wallis test) was used, followed by a post-hoc Mann–Whitney test [29].

3. Results and Discussion

3.1. Effect of pH on phosphate and ammonium removal

The results revealed that the pH significantly affected the efficiency of phosphate removal in the electrocoagulation process using a magnesium anode. Phosphate decreased by 1.41, 1.68, and 2.26 mg/L at pH 7; the phosphate reduction increased at pH 8, where reductions of 4.37, 4.79, and 4.63 mg/L were observed with current applications of 3A, 5A, and 10A, respectively. Meanwhile, at pH 9, there was a decrease in phosphate removal, with reductions of 2.20, 3.28, and 3.45 mg/L at the same currents, as shown in Table S2–S4. At pH 8, the highest efficiency of 91.27% ± 4.15 was achieved at a current of 5 A (Figure 2). This indicates that this pH is optimal for the electrocoagulation process using a magnesium anode. This indicates that the effect of pH is more dominant than the increase in electric current, as the phosphate removal pattern still reaches its maximum value at pH 8 for all current variations. In addition, the relatively low standard deviation at 3 and 5 A (<5%) indicates that this process is quite stable and has good reproducibility, whereas the increase in the standard deviation at 10 A shows that an excessively high current leads to the formation of less stable flocs owing to an excessive magnesium dissolution rate. Overall, pH 8 is the optimum condition for this system, especially in the context of continuous operation and the use of Mg electrodes [30,31]. At this pH, there is a synergy between Mg^{2+} release, $Mg(OH)_2$ formation, and struvite precipitation, which results in maximum phosphate recovery while maintaining ammonium in a controlled phase [32].

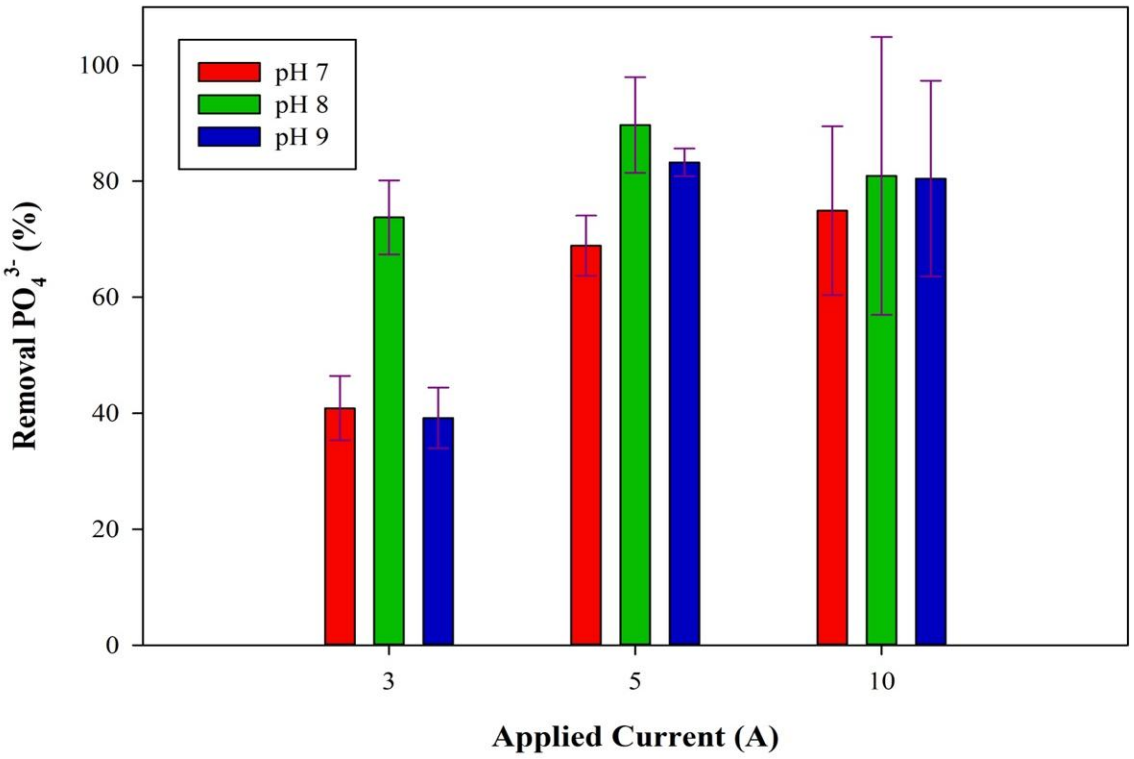


Figure 2. Removal of phosphate during electrocoagulation using a Mg anode

As shown in Figure 2, at pH 7, the formation of $Mg(OH)_2$ was not optimal; thus, the amount of active floc remained limited, and the removal efficiency was relatively low. Conversely, at pH 9, the excessively high concentration of OH^- ions led to changes in floc characteristics through agglomeration and a decrease in effective surface area, as well as increased competition between OH^- ions and phosphate for adsorption sites. This mechanism has been widely applied to remove anions, such as phosphate and metal contaminants, from various types of wastewater, yielding promising results in terms of removal efficiency and process [33].

Therefore, the high phosphate removal efficiency achieved at pH 8 not only demonstrates the optimal conditions for $Mg(OH)_2$ floc formation but also indicates the possibility of simultaneous ammonium removal via struvite precipitation. This mechanism makes magnesium-based EC technology effective in reducing nutrient loads and supporting the concept of nutrient recovery in sustainable wastewater treatment. Conversely, pH 7 was insufficient to effectively support precipitate formation, whereas pH 9 tended to cause reaction imbalances owing to the competition between hydroxide and ammonia volatilisation. These findings confirm that in the design of continuous-mode magnesium-based electrocoagulation systems, pH control within a slightly alkaline range is crucial for achieving optimal and stable nutrient recovery [30,31,34]. In addition

to increasing efficiency, operation at the optimum pH also supports the formation of value-added products, such as struvite, thereby providing additional potential within the resource recovery concept from wastewater [33,35].

The pH showed a positive trend with respect to the ammonium removal efficiency using magnesium magnesium electrode-based electrocoagulation, although this trend was not statistically significant, as shown in Figure 3 and Tables S5-S7. The average ammonium removal efficiency increased from 52.37% at pH 7 to 68.76% at pH 8, and then slightly decreased to 67.93% at pH 9. The highest efficiency was recorded at 71.46% at pH 9 with currents of 5 and 10 A, whereas the lowest efficiency was achieved at pH 7 with the same currents (48.23 %).

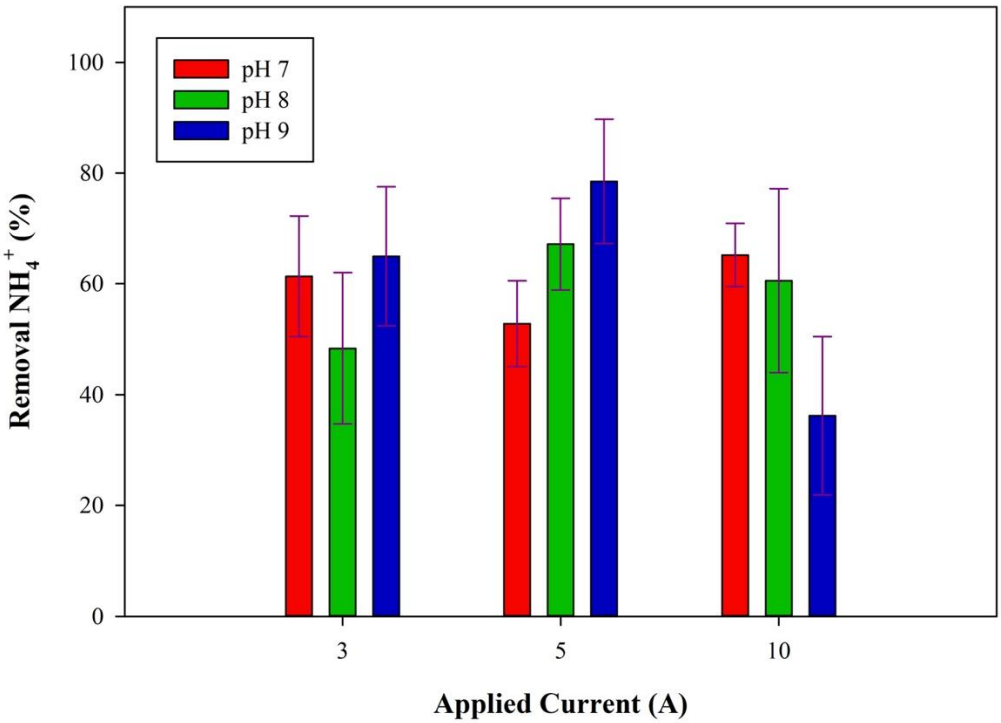


Figure 3. Removal of ammonium during Mg anode electrocoagulation

Overall, increasing the pH from neutral to alkaline enhanced the removal of both phosphate and ammonium, although the effect was more pronounced for phosphate removal. The higher phosphate removal at pH 8–9 can be attributed to the increased availability of Mg^{2+} released from the magnesium electrode and the formation of $Mg(OH)_2$ flocs, which facilitate the adsorption and precipitation of phosphate. Simultaneously, Mg^{2+} can react with NH_4^+ and PO_4^{3-} to form struvite ($MgNH_4PO_4 \cdot 6H_2O$), providing a coupled mechanism for simultaneous phosphate and ammonium removal. Thus, the higher ammonium removal observed under alkaline conditions is not only

associated with the increased conversion of NH_4^+ to NH_3 but also with enhanced struvite formation, particularly within the pH range of 8–9, as reported in previous studies [36,37].

However, the increase in ammonium removal was less pronounced than that of phosphate, indicating that phosphate availability remained a limiting factor for struvite formation in the wastewater. Increasing the current from 5 to 10 A did not consistently improve ammonium removal at pH 8–9, despite the higher rate of magnesium dissolution. Excessive Mg^{2+} release can promote rapid $Mg(OH)_2$ formation and floc agglomeration, reducing the effective surface area and destabilising the flocs through erosion or fragmentation [38], [39]. The relatively low variation in the standard deviation (<7.5%; Tables S5–S7) indicates that the process remained consistent across the operating conditions. These results suggest that pH is the dominant parameter governing nutrient removal, whereas current primarily controls magnesium dissolution and floc formation. Accordingly, a pH of 8–9 provided the most favourable balance between $Mg(OH)_2$ formation, struvite precipitation, and ammonium conversion, establishing an effective operating window for simultaneous phosphate and ammonium removal [40].

In addition to its effect on nutrient removal, the initial pH also influenced the pH evolution during magnesium electrocoagulation. As shown in Figure 4, the effluent pH increased under all operating conditions, indicating the progressive alkalinization of the solution during the electrochemical process. The increase was most pronounced at an initial pH of 7, where the effluent pH increased from approximately 9.6 at 3 A to 10.1 at 10 A. This trend indicates that increasing the current intensity enhances the electrochemical reactions responsible for hydroxide generation and magnesium dissolution, thereby promoting a more alkaline reaction environment. In contrast, at initial pH values of 8 and 9, the effluent pH remained relatively close to 10, regardless of the applied current, suggesting that the system approached a relatively stable alkaline condition. The smaller differences among current levels at higher initial pH values may indicate that the contribution of additional current to further pH elevation became progressively limited once sufficient alkalinity was established. Therefore, the observed pH evolution demonstrates that the current intensity primarily affects the rate of alkalinization at a lower initial pH, whereas the initial pH determines the overall chemical environment in which magnesium hydrolysis, $Mg(OH)_2$ formation, and nutrient precipitation occur. This behaviour is important for continuous magnesium electrocoagulation because excessive alkalinization may shift the process away from the optimum

conditions for nutrient recovery, even when a higher current promotes greater electrode dissolution.

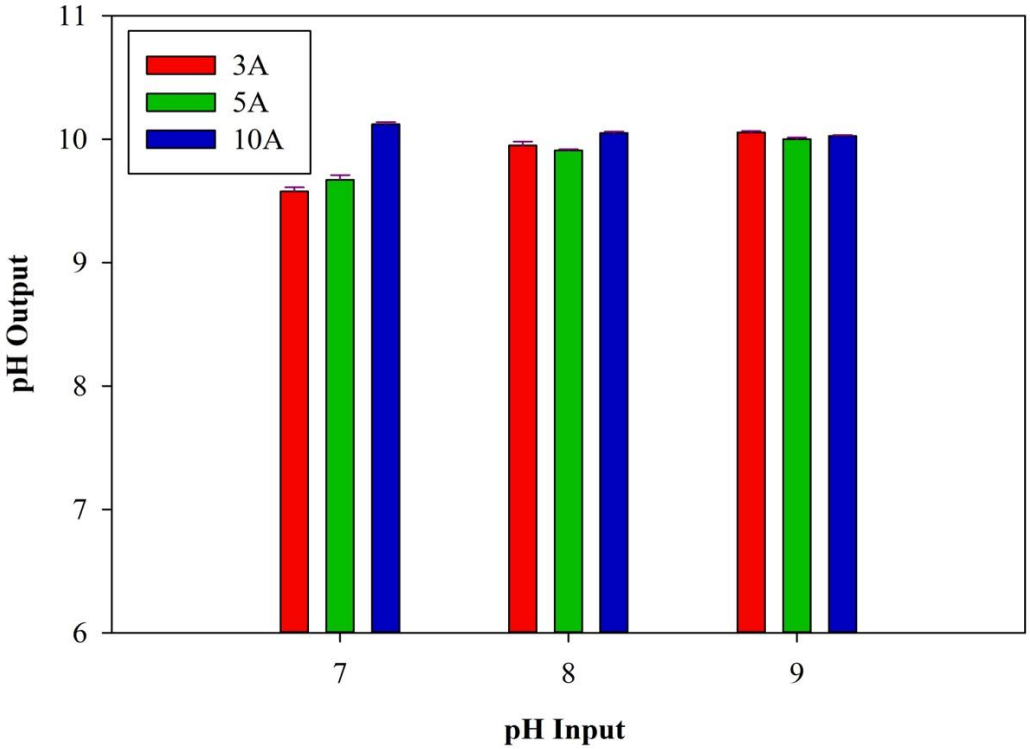


Figure 4. pH evolution during Mg anode electrocoagulation

3.2.Effect of applied current on phosphate and ammonium removal

The application of current determines the rate of Mg^{2+} ion release and the formation of $Mg(OH)_2$ coagulant, which subsequently affects the rate of struvite precipitation and the removal of NH_4^+ and PO_4^{3-} from wastewater. The influence of current was assessed at three distinct levels (3, 5, and 10 A) under pH conditions of 7, 8, and 9 to examine the relationship between current intensity, pH conditions, and nutrient recovery efficiency. The results indicate that increasing the current from 3 A to 5 A generally increases the efficiency of phosphate and ammonium removal, as shown in Figures 2 and 3, respectively. These results are consistent with those of previous studies on COD reduction after the electrocoagulation process [41], microplastics [42], and increased efficiency in ammonium reduction [43]. Further increases up to 10 A did not provide a significant performance improvement and even reduced the efficiency under certain conditions, as discussed previously.

In the phosphate removal process, the highest efficiency recorded was 91.27% when the pH was 8 and the current was set at 5 A. However, the efficiency decreased to 88.28% when the

current was increased to 10 A. A similar pattern was observed for ammonium removal; at pH 8, the efficiency rose from 67.29% at a current of 3 A to 69.50% at 5 A, but no further increase was observed when the current reached 10 A. At pH 9, the ammonium efficiency reached 71.46% at both 5 and 10 A, indicating that increasing the current beyond 5 A no longer enhanced the nutrient removal capacity. These findings indicate that the optimal current is approximately 5 A, as it can generate sufficient coagulant without disrupting the floc stability. The results of this study are also consistent with those of previous studies on the electrocoagulation process using iron and magnesium electrodes to reduce phosphate [44].

As shown in Figures 2 and 3, increasing the current from 3 to 5 A increased Mg dissolution from 1.34 to 2.23 g and increased phosphate reduction at pH 8 from 0.52 to 0.56 g, whereas ammonium reduction increased more markedly from 3.02 to 3.72 g. Further increasing the current to 10 A, although resulting in Mg dissolution up to 4.47 g, did not proportionally enhance phosphate or ammonium reduction; phosphate reduction at pH 8 slightly decreased to 0.53 g, while ammonium reached 3.66 g (Figure 5).

In Figure 5, increasing the electrochemical Mg addition does not always correlate linearly with the treatment performance, as higher currents intensify OH^- formation, causing more Mg^{2+} to transform into $Mg(OH)_2$, which can increase the competition between hydroxide floc and struvite formation. At pH 8, alkalinity conditions supported the presence of Mg^{2+}, NH_4^+, and PO_4^{3-} in more suitable conditions for struvite precipitation, thus providing the highest phosphate reduction along with relatively high ammonium reduction. Conversely, at pH 7, limited OH^- and phosphate speciation make struvite formation less optimal, whereas at pH 9, increasing the pH does not provide significant improvement, and phosphate reduction is lower, possibly due to dominant $Mg(OH)_2$ formation as well as changes in phosphate speciation. The increased efficiency of phosphate removal at pH 8 is closely linked to the in-situ formation of $Mg(OH)_2$ flocs from the magnesium electrode, which is well known to provide high efficiency in the adsorption of anionic ions, such as phosphate. The in situ formation of $Mg(OH)_2$ produces highly active flocs with a large effective surface area, enhancing the adsorption of phosphate and ammonium and facilitating their subsequent precipitation [45].

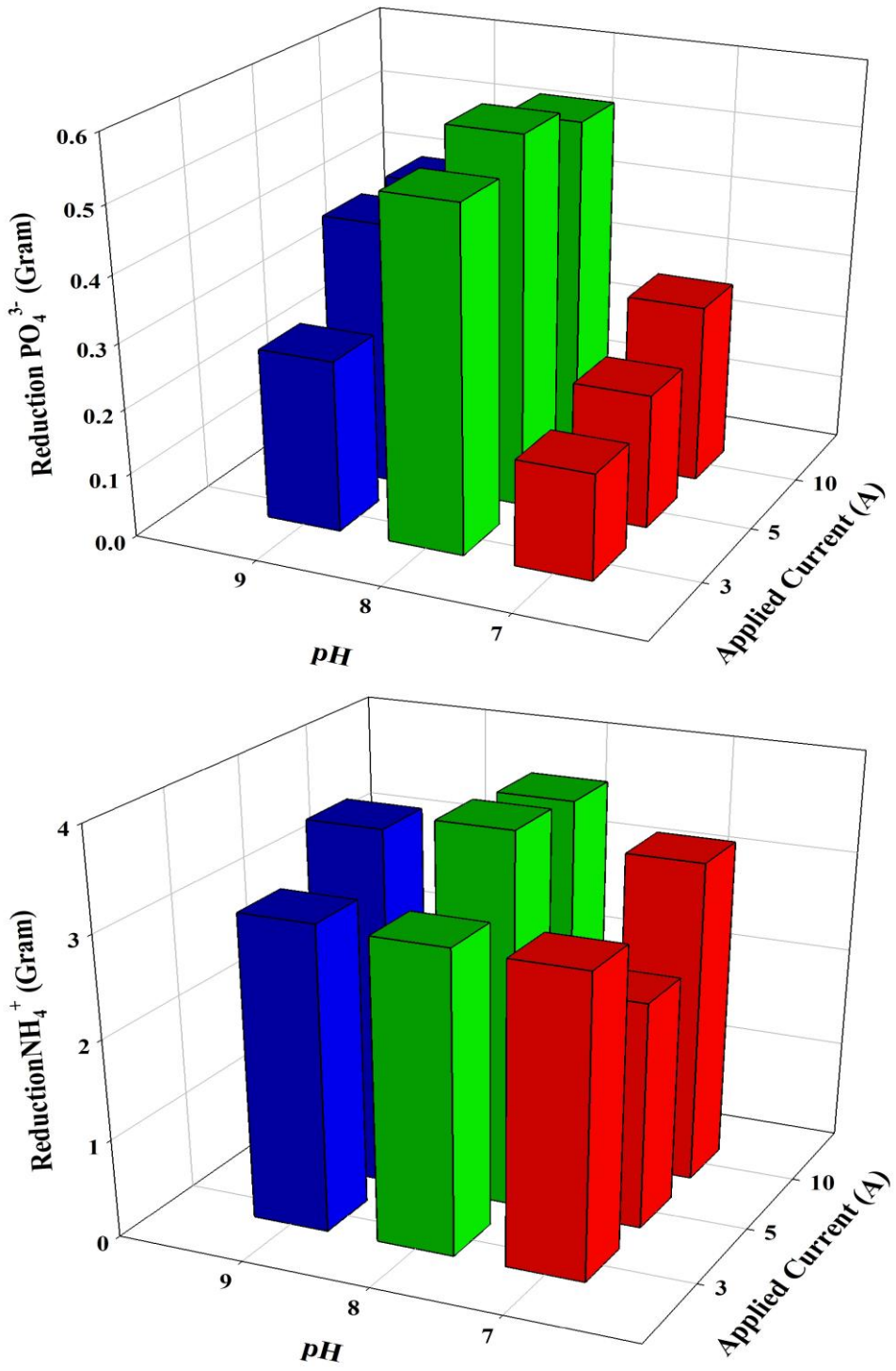


Figure 5. Phosphate and Ammonium Reduction During Mg Anode Electrocoagulation

The relationship between ammonium reduction accumulation and energy consumption indicates a trade-off between the increased removal capacity and energy requirements of the EC-

Mg process. At a current of 3 A (Table 2), the energy consumption was relatively low, averaging approximately 0.18, 0.19, and 0.26 kWh/m³ at pH 7, 8, and 9, respectively, but the mass of reduced NH_4^+ remained relatively limited. Increasing the current to 5 A raised the energy consumption to approximately 0.43, 0.44, and 0.60 kWh/m^3 at pH 7, 8, and 9, respectively, which was accompanied by increased accumulation of ammonium reduction owing to the greater release of Mg^{2+} and floc formation that facilitates NH_4^+ binding and precipitation through struvite formation. However, at a current of 10 A, energy consumption rises sharply to approximately 1.36 kWh/m^3 at pH 7, 2.12 kWh/m^3 at pH 8, and 2.55 kWh/m^3 at pH 9, while the increase in ammonium reduction is no longer proportional to the additional energy supplied. Thus, higher currents can achieve greater ammonium reduction capacity but with significantly higher energy consumption. From a process efficiency perspective, the pH 8–5 A condition potentially offers a better compromise between ammonium reduction, reaction rate, and energy consumption, whereas pH 8–10 A is more appropriate when the main priority is to maximise the removal capacity rather than energy efficiency.

Table 2. Energy consumption and current density during electrocoagulation with Mg anode

pH	Applied current (A)	Energy consumption (kWh/m^3)	Current density (A/m^2)
7	3	0.18 ± 0.01	47.7
	5	0.43 ± 0.01	79.6
	10	1.36 ± 0.22	159.2
8	3	0.19 ± 0.01	47.7
	5	0.44 ± 0.01	79.6
	10	2.12 ± 0.01	159.2
9	3	0.26 ± 0.01	47.7
	5	0.60 ± 0.03	79.6
	10	2.54 ± 0.42	159.2

3.3.Effect of the Mg electrocoagulation on TSS reduction

The influent TSS concentration under all test conditions was relatively uniform at approximately 128–129 mg/L, as shown in Figure 5. After the electrocoagulation process, a significant decrease in TSS was observed across all pH and current variations, indicating that the

electrocoagulation process effectively reduced suspended particles through colloid destabilisation, floc formation, and solid separation mechanisms. At a current of 3 A, the effluent TSS concentrations reached approximately 34, 28 mg/L at pH 8, and 53 mg/L at pH 7, 8, and 9, respectively. The pH 8 condition produced the best performance with the lowest TSS concentration and a removal efficiency of approximately 78%, while the pH 9 condition showed the lowest efficiency of approximately 59%, as shown in Figure 6.

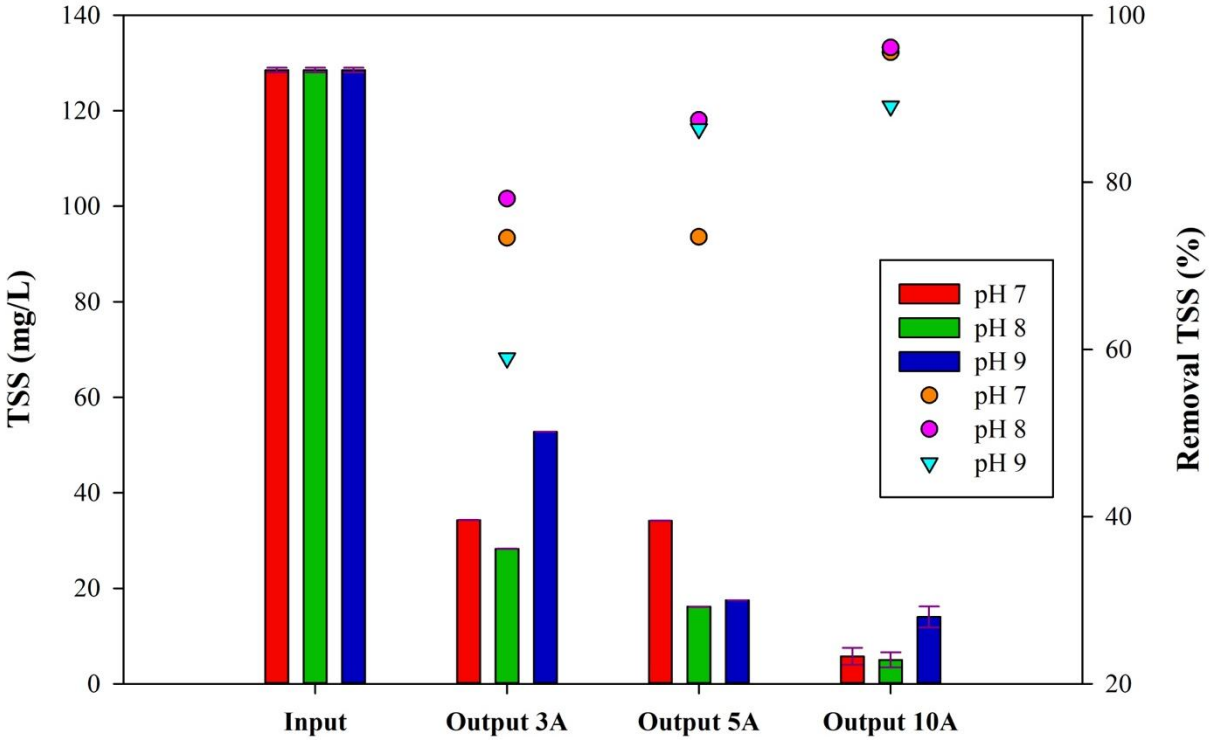


Figure 6. Reduction of TSS during electrocoagulation using an Mg anode

As shown in Figure 6, excessively high alkaline conditions do not necessarily enhance the coagulation process because the formation of hydroxide species and floc characteristics can change at higher pH values. Increasing the current to 5 A resulted in a greater reduction in TSS, especially at pH 8 and 9. The TSS concentrations decreased to approximately 16 and 17 mg/L, respectively, with removal efficiencies of approximately 87% and 84%. At pH 7, the TSS concentration remained at approximately 34 mg/L; therefore, increasing the current did not result in a significant change compared to the 3 A condition. This phenomenon indicates that the effectiveness of increasing the current depends on the pH conditions, as the chemical conditions of the solution influence the formation of in-situ coagulants and floc characteristics. At a current of 10 A, the TSS concentration decreased to approximately 6 mg/L at pH 7, 5 mg/L at pH 8, and 14 mg/L at pH 9.

The removal efficiencies were approximately 95%, 96%, and 90%, respectively. Thus, the combination of pH 8 and a current of 10 A provided optimum performance, resulting in the lowest final TSS and the highest removal efficiency. However, this condition needs to be further evaluated in terms of energy and electrode consumption to determine operating conditions that are not only technically effective but also economically and environmentally optimal for the process.

3.4. Potential struvite characteristics

Based on the SEM–EDX results at pH 8 and 5 A (Figure 7), the precipitates exhibited elongated, rod-like, and prism-shaped crystals with relatively sharp edges and an irregular surface. This morphology is consistent with previously reported struvite crystals formed from liquid waste, which commonly exhibit rod-like, coffin-like, or elongated morphologies with relatively rough surfaces [36,50]. At 10 A, the crystals retained an elongated morphology but appeared larger and denser, with a more pronounced prism- or tube-like structure. This morphology may indicate the formation of a more alkali-rich phase, such as hazenite, which can develop under conditions with elevated Mg and alkali metal concentrations. Elemental mapping revealed that Mg, P, and O were the predominant elements within the crystals, supporting the formation of magnesium phosphate-based precipitates. The absence of N in the EDX spectra does not necessarily exclude struvite formation because EDX has limited sensitivity toward light elements, particularly N and H, whose low-energy X-ray signals can be masked by the stronger signals from heavier elements. Overall, the pH 8–5 A condition produced crystals with a morphology and elemental composition indicative of relatively pure struvite, whereas the pH 8–10 A condition appeared to promote the formation of larger, denser crystals with a greater contribution from alkali-rich phases, suggesting the possible coexistence of struvite and hazenite.

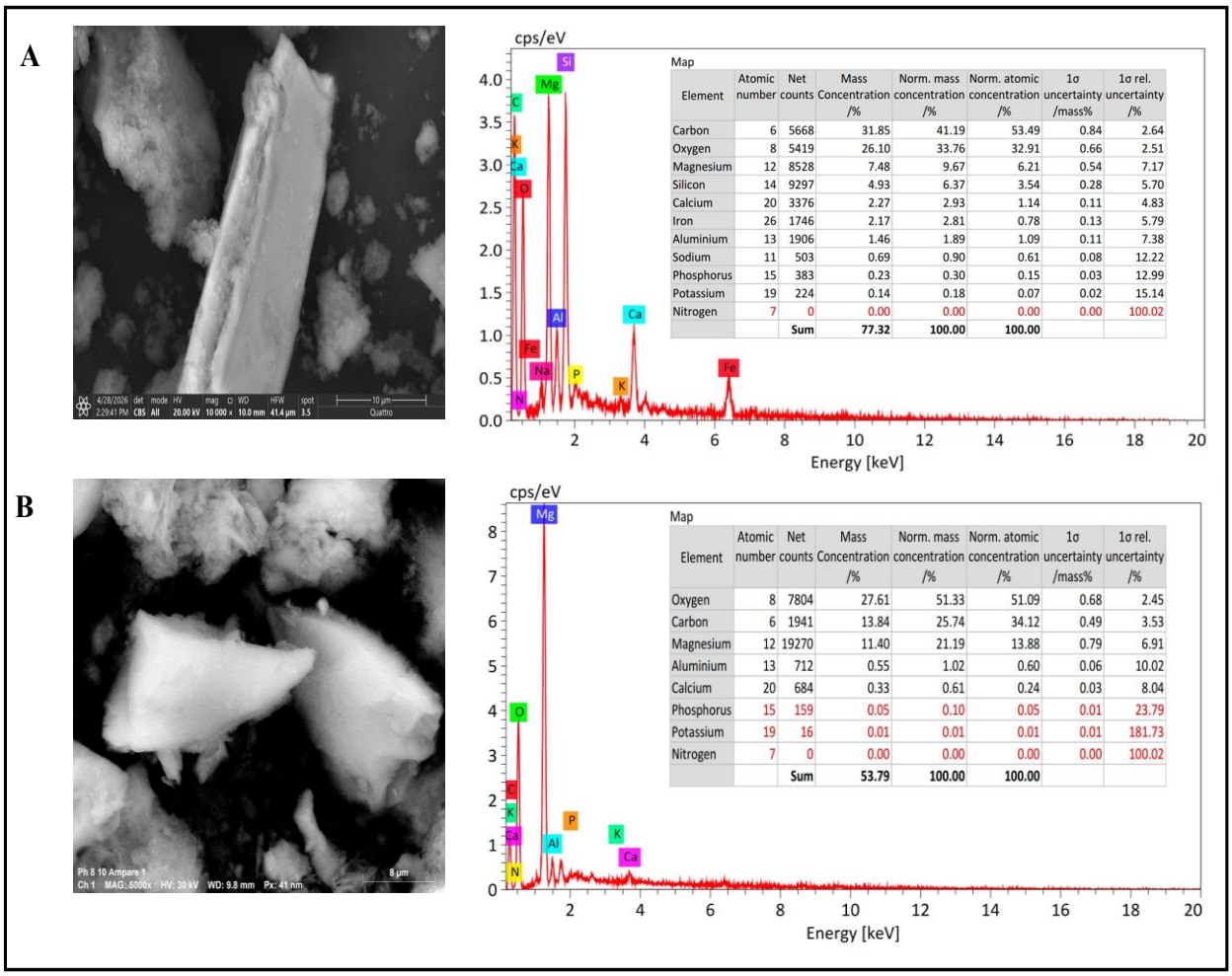


Figure 7. SEM-EDX analysis results at pH 8 (A. Applied current 5A, B. Applied current 10A)

The characterisation of wastewater in this study focused on samples obtained under operating conditions of pH 8 with currents of 5 and 10 A, as these two combinations showed a tendency to provide the highest recovery efficiency for NH_4^+ and PO_4^{3-} in previous studies. The samples were characterised using XRD to identify the crystalline phases formed in the precipitate resulting from the electrocoagulation process and to confirm the presence of struvite as the main product. Based on the XRD diffractogram in Figure 8, the sample exhibited 12 peaks at 21.025°, 21.916°, 26.551°, 29.352°, 34.961°, 36.613°, 55.484°, 55.661°, 56.214°, 59.214°, 59.733°, 60.554°, and 65.697° at pH 8 with a current of 5 A. Under the 10A condition, there were nine peaks at 15.347°, 20.607°, 29.152°, 30.853°, 31.777°, 38.056°, 47.162°, 58.824°, and 67.357°, most of which corresponded to the characteristic peaks of hazenite and struvite reported in the literature. Peaks in the ranges of 20°–22°, 29°–31°, and approximately 35°–38° are strong indications of struvite [46,47]. Next,

pattern matching analysis was performed using Match! 2.0 was used to interpret these peaks. The mineral phase identification results are shown in Figure S1.

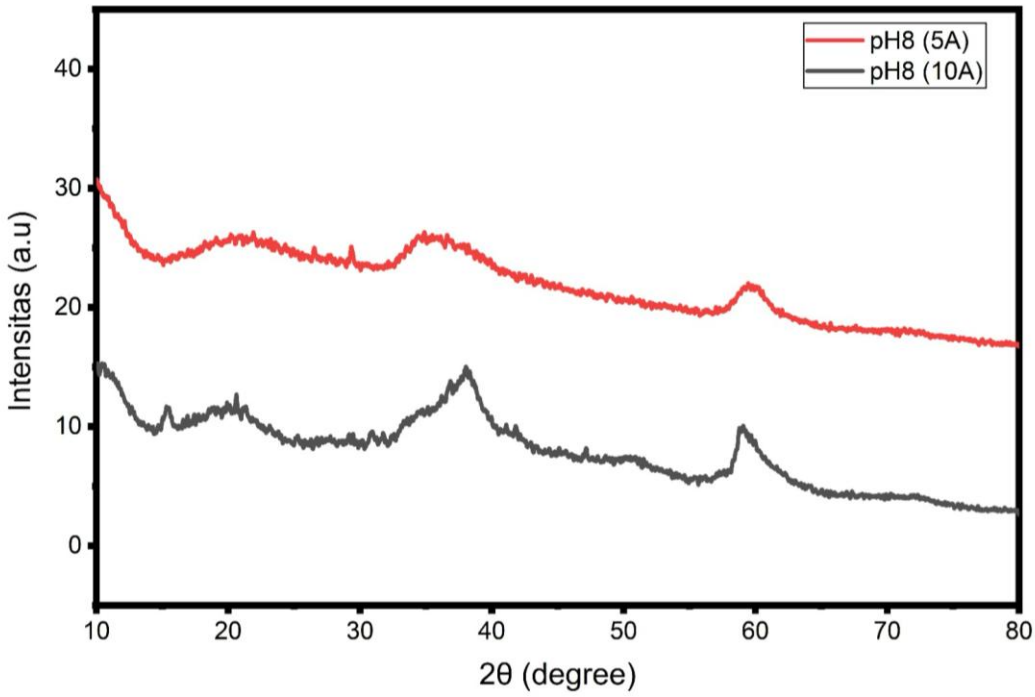


Figure 8. Struvite diffractogram at pH 8 with 5 and 10 A applied current

Based on the Match! 2.0 result (Figure S1 and S2), the crystal found in the product is amenite at 32.4% with the formula $KNaMg_2(PO_4)_2.14H_2O$. Hazenite is a hydrated phosphate mineral belonging to the struvite group, with two monovalent cations (Na^+ and K^+) that partially substitute for NH4+ in its crystal structure. Hazenite forms under phosphate- and magnesium-rich conditions with an alkaline pH and can be synthesised from various Mg and Na sources, including nutrient-rich wastewater [48]. The presence of hazenite crystals in the largest quantity in this sample indicates that operating conditions of pH 8 with a current of 5A not only support the formation of struvite but also facilitate cation substitution by Na^+ or K^+ from the wastewater, resulting in struvite derivatives rich in alkali elements. The next crystals formed are struvite ($NH_4MgPO_4.6H_2O$) with a fraction of 24.3% identified through the matching of characteristic struvite peaks in the XRD pattern with reference data, particularly in the range 2θ around 21-22°, 29-31°, and 35-37°. The presence of a relatively large amount of struvite aligns with the results of the previous process, in which at pH 8 and a current of 5A, the concentrations of NH_4^+ and PO_4^{3-} decreased sharply with a high recovery percentage, strongly indicating that most of these nutrients were removed through

the formation of struvite and its derivatives. In addition to these two crystals, brucite ($Mg(OH)_2$) was also present at 9.3% in the sample. Brucite commonly forms during the electrocoagulation process with a magnesium anode as dissolved Mg^{2+} ions react with OH^- generated near the anode or due to increased pH, resulting in the precipitation of $Mg(OH)_2$, which functions as a coagulant.

Match! 2.0 analysis at pH 8 with a current of 10 A also showed that the crystals formed were 36.5% amenite ($KNaMg_2(PO_4)_2.14H_2O$), 18.5% struvite ($NH_4MgPO_4.6H_2O$), and 9,8% brucite ($Mg(OH)_2$). This indicates that an increase in current will shift the solid composition toward struvite derivatives rich in K+ or Na+ cations, while the proportion of pure struvite will decrease, although it is still clearly detected. Based on the XRD analysis results, in addition to struvite, an amenite phase was formed ($KNaMg_2(PO_4)_2.14H_2O$). Hazenite is a hydrated phosphate mineral belonging to the struvite group, but with K^+ and Na^+ as the monovalent cations forming its structure, in contrast to struvite which contains NH_4^+. The presence of this phase indicates that during the electrocoagulation process, there is competition among NH_4^+, K^+, and Na^+ to associate with Mg^{2+} and phosphate. Mg^{2+} ions were released in situ from the magnesium anode, whereas K^+ and Na^+ may originate from the domestic wastewater matrix and pH adjustment using NaOH. A slightly alkaline pH and the simultaneous availability of Mg^{2+}, phosphate, K^+, and Na^+ subsequently promoted amenite formation as a coprecipitation phase. A similar phenomenon was studied by [49], who found that the presence of Na^+ in the solution and the use of NaOH during the pH adjustment stage resulted in the formation of hazenite, alongside K-struvite. Under pH 8 conditions with a current of 5 A, XRD pattern matching showed an amenite fraction of 32.4%, which was higher than that of struvite at 24.3%. When the current was increased to 10 A, the amenite fraction increased to 36.5%, whereas the struvite fraction decreased to 18.5%.

This trend indicates that increasing the current accelerates anode dissolution and increases the availability of Mg^{2+} but does not selectively enhance struvite formation. In a system where phosphate acts as the limiting reagent and both K^+ and Na^+ are present, excess Mg^{2+} can participate in the formation of amiantite and brucite. Therefore, the dominance of hazenite at 10 A explains that increasing the current beyond the optimum condition not only potentially leads to excessive floc formation but also shifts the product phase distribution from struvite to Mg–Pa–SP minerals. Although the formation of hazenite reduces the selectivity for struvite formation, this phase still has value as a nutrient recovery product because it contains phosphorus, potassium, and magnesium, which could potentially be used as mineral fertilisers. However, because ammonite

does not contain ammonium, the dominance of this phase indicates that not all nitrogen is recovered in the solid product.

Based on the FTIR spectrum (Figure 9), a broad absorption band was observed in the high wavenumber region (approximately 3700–3200 cm^{-1}) originating from the O–H stretching vibrations of hydrated water molecules bonded by hydrogen within the crystal structure, which also overlaps with the N–H stretching from NH_4^+.

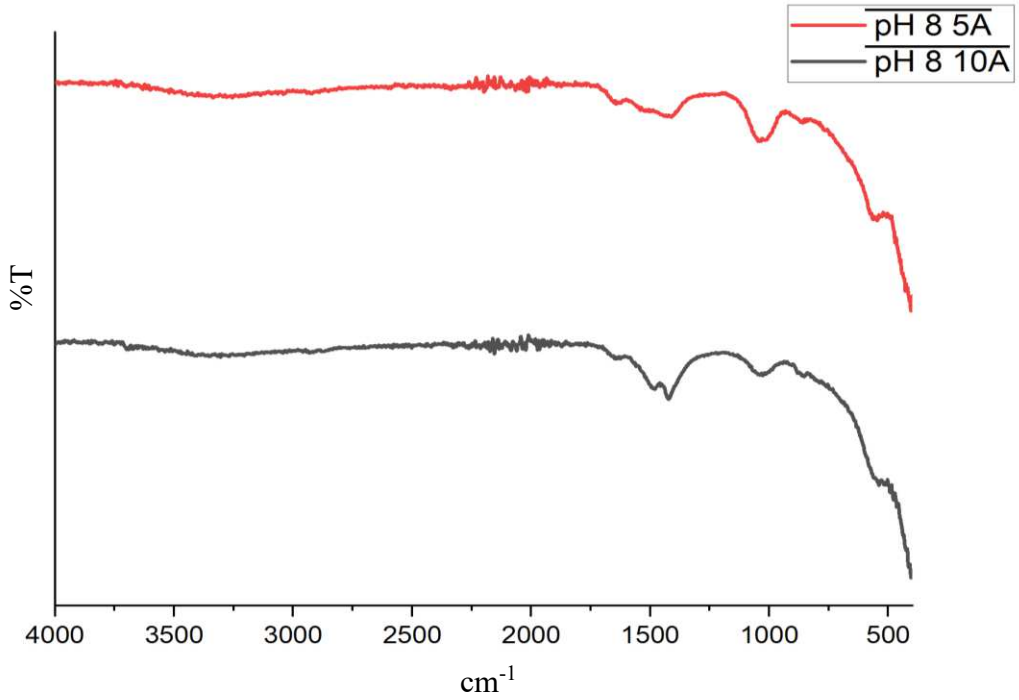


Figure 9. FTIR spectra at pH 8 with 5A and 10A

The broadband pattern in FTIR spectra area is consistent with the results of a previous study [50], which stated that the combination of O–H and N–H vibrations produces several overlapping spectral components, thus appearing as a single broad band characteristic of struvite. The N–H spectrum position at 1480-1410 cm^{-1} is consistent with the results [50], which indicates that the m4 (NH_4^+) mode in struvite splits into two to three components in the 1440–1480 cm^{-1} range owing to the decrease in NH_4^+ ion symmetry from Td to Cs and the influence of correlation fields within the lattice. In the region between 1035–1025 cm^{-1} and in the range of 850–860 cm^{-1} as well as 500–600 cm^{-1}, these can be interpreted as the vibrational modes v_3 (PO_4^{3-}) and v_4/v_2 (PO_4^{3-}). Based on the conformity of the FTIR spectral pattern, which includes the O–H/N–H stretching band in the high-frequency region, the H–O–H and N–H bending bands in the mid-wavenumber region, and the phosphate band system v_3 and v_4/v_2 (PO_4^{3-}). In the fingerprint region, within the same

range as the reference struvite spectrum, the phase is magnesium ammonium phosphate hexahydrate struvite ($NH_4MgPO_4.6H_2O$) formed in the deposits resulting from wastewater treatment.

3.5.Statistical Analysis

The Kruskal–Wallis test revealed that the ammonium removal efficiency data did not conform to a normal distribution ($p = 0.024 < 0.05$). Consequently, a non-parametric statistical method was chosen to assess the impact of changes in pH and current intensity on the process performance. The test results showed that variation in pH did not have a significant effect on ammonium removal ($H = 4.73$; $p = 0.094 > 0.05$); therefore, the null hypothesis (H_0) was accepted. However, the descriptive statistical analysis indicated that pH 8 yielded the highest median ammonium removal at 64.35% with a mean rank of 44.1, compared with pH 7 (61.42%; mean rank 32.7) and pH 9 (59.11%; mean rank 32.8). This suggests that pH 8 provided the best performance, even though the increase was not statistically significant. Electrochemically, a near-neutral to slightly alkaline pH supports the formation of more stable metal hydroxide flocs $Mg(OH)_2$, enabling the effective adsorption and entrapment of ammonium. However, because the mechanism of ammonium removal in electrocoagulation is more influenced by adsorption and coprecipitation than by direct chemical reactions, changes in pH in the range of 7–9 did not result in significant differences in efficiency. In contrast, current intensity had a significant effect on ammonium removal efficiency, with $H = 8.07$ and $p = 0.018$ (<0.05); therefore, the null hypothesis was rejected, and a significant difference between current treatments was concluded. Based on the median and mean rank values, a current of 5 A provided optimal performance, with a median removal of 66.78% and a mean rank of 42.7, which was higher than those at 3 A (61.45%; mean rank 40.1) or 10 A (57.10%; mean rank 26.7). These results show that increasing the current to 5 A can enhance anode dissolution and the optimal formation of coagulant species, thus increasing the number of flocs formed and improving the adsorption capacity for ammonium. However, further increasing the current to 10 A decreased the removal efficiency. This phenomenon may be due to the excessively rapid formation of hydrogen and oxygen bubbles, which disrupt floc agglomeration, increase reactor turbulence, and reduce the contact time between flocs and the ammonium ions. In addition, excessively high currents increase energy consumption without correspondingly increasing the treatment efficiency. Therefore, these results confirm that a current of 5 A is the most optimal operating condition for the electrocoagulation process in removing ammonium, whereas pH

optimisation in the range of 7–9 does not have a statistically significant effect, although pH 8 tends to yield the highest efficiency.

4. Conclusion

This study showed that EC-Mg effectively removed phosphate and ammonium from domestic wastewater and could aid in nutrient recovery. The success of this process depends on the interaction between the pH and electric current. A pH of 8 was ideal for phosphate removal, achieving up to 91.27 ± 4.15% efficiency at a current of 5 A. Ammonium removal was more complex and was more affected by the current than by pH, with the best results at 5 A. Increasing the current from 3 to 5 A increased Mg dissolution and coagulant formation, improving nutrient reduction. However, increasing the current to 10 A did not proportionally increase ammonium removal and could reduce its efficiency.

This suggests that excess Mg^{2+} and $Mg(OH)_2$ formation can cause floc agglomeration and competition between Mg hydroxide formation and phosphate struvite precipitation. The ammonium rate constant decreased from 0.0788 to 0.0688 and 0.0497 min^{-1} as the current increased from 3, 5, and 10 A, respectively. Energy consumption at pH 8 increased from approximately 0.20 kWh/m^3 at 3 A to 0.44 kWh/m^3 at 5 A and over 2.1 kWh/m^3 at 10 A. Thus, pH 8–5 A offered a better balance between removal efficiency, and energy use, while pH 8–10 A was better for maximising TSS removal, reaching approximately 96%. Precipitate analysis using XRD, SEM-EDX, and FTIR confirmed the formation of a struvite phase and related minerals, with the composition at pH 8–5 A being approximately 24.3% struvite, 32.4% hazenite, and 9.3% brucite. Increasing the current to 10 A increased the ammonite fraction to 36.5% and decreased the struvite fraction to 18.5%. Thus, increasing the electrochemical intensity does not necessarily enhance struvite selectivity but can shift precipitation toward other magnesium-phosphate phases because of phosphate limitations and the presence of K^+ and Na^+ ions. Overall, a pH of 8 and a current of 5 A were the most balanced conditions for a continuous EC-Mg system, achieving high nutrient removal with lower energy consumption compared to 10 A and still resulting in struvite.

These findings suggest that the development of EC-Mg as a nutrient recovery technology should focus on balancing the removal efficiency, reaction rate, energy and electrode use, floc stability, and the selectivity and quality of the recovered product. For development, the integration of wastewater with high phosphate content, particularly with livestock wastewater, fertiliser

industry, and agro-industry wastewater in general, is highly feasible, enabling the creation of a circular economy.

Acknowledgements

This research was financially supported by the National Research and Innovation Agency (BRIN) under Grant No. 106/II.7/HK/2026, for the Research and Innovation Programs for Indonesia Advance (11th Batch Competition).

Author contributions

Yulisya Zuriatni: Writing, original draft, reviewing and editing, resources, funding acquisition, and data curation. **Gani Purwiandono**: methodology, conceptualization. **Rachmad Ardhianto:** writing, editing, methodology, conceptualization. **Nurcahyo Iman Prakoso:** reviewing and editing. **Tatang Shabur Julianto:** reviewing and editing.

Conflicts of interest

There are no conflicts of interest to declare.

Data availability

The datasets used and analysed in this study are available upon request from the corresponding author.

Declaration of generative AI and AI-assisted technologies in the preparation of the manuscript.

During the preparation of this work, the author(s) used Paperpal to enhance the clarity, flow, and readability of the text. After using this tool/service, the author(s) reviewed and edited the content as needed and took full responsibility for the content of the published articles.

Reference

[1] T.-M.-T. Le, T.-T. Nguyen, T.-A. Nguyen, T.-H.-T. Nguyen, P.-D. Nguyen, Water Quality Assessment of Urban Canals in Ho Chi Minh City, Vietnam: Effectiveness of Renovation Efforts in Minimizing Pollution, Journal of Water Management Modeling (2025). https://doi.org/10.14796/jwmm.s545.

[2] F. Li, J. Li, Z. Ren, Impact of Ecological Engineering on Water Quality Improvement under Urbanization: A Case Study in Xiaoqing River in Jinan, China, Environmental Challenges 20 (2025) 101260. https://doi.org/10.1016/j.envc.2025.101260.

[3] H. He, K. Chen, Y. Du, K. Li, Z. Liu, E. Jeppesen, M. Søndergaard, Increased Nitrogen Loading Boosts Summer Phytoplankton Growth by Alterations in Resource and Zooplankton Control: A Mesocosm Study, Front. Environ. Sci. 9 (2021). https://doi.org/10.3389/fenvs.2021.772314.

[4] Y. Kim, D. Kim, Y.-O. Kim, M. Son, B. Lee, S.H. Baek, Threshold-based analysis of eutrophication dynamics in a semi-enclosed bay: The dominant role of dissolved inorganic nitrogen in Masan Bay, South Korea (2010-2015)., Mar. Pollut. Bull. 222 (2026) 118657. https://doi.org/10.1016/j.marpolbul.2025.118657.

[5] R. Ghosh, A. Basu, A. Ghosh, INDUSTRIAL WASTEWATER AS A FEEDSTOCK FOR GREEN HYDROGEN PRODUCTION: TOWARDS CIRCULAR ECONOMY AND SUSTAINABILITY, RASAYAN Journal of Chemistry 18 (2025) 1401–1413. https://doi.org/10.31788/rjc.2025.1839195.

[6] S. Maremane, G. Belle, P. Oberholster, Assessment of Effluent Wastewater Quality and the Application of an Integrated Wastewater Resource Recovery Model: The Burgersfort Wastewater Resource Recovery Case Study, Water (Basel). 16 (2024) 608. https://doi.org/10.3390/w16040608.

[7] R. Mores, A. Cunha Junior, F.G. Antes, M. Di Luccio, C.E.D. Oro, M. V Tres, C. Steffens, J. Steffens, A. Kunz, R.M. Dallago, Electrochemical Precipitation of Struvite from Wastewater: A Sustainable Approach for Nitrogen Recovery, Separations 12 (2025) 108. https://doi.org/10.3390/separations12050108.

[8] Z. Isik, B. Caliskan, P. Belibagli, N. Dizge, Investigation of optimum conditions for the recovery of magnesium ammonium phosphate from human urine using the Box–Behnken design, Water Practice & Technology 19 (2024) 3009–3021. https://doi.org/10.2166/wpt.2024.169.

[9] I. Wu, J.D. Hostert, G. Verma, M.-C. Kuo, J.N. Renner, A.M. Herring, Electrochemical Struvite Precipitation Enhanced by an Amelogenin Peptide for Nutrient Recovery, ACS Sustainable Chemistry & Engineering 10 (2022) 14322–14329. https://doi.org/10.1021/acssuschemeng.2c04691.

[10] L. Kékedy-Nagy, A. Teymouri, A.M. Herring, L.F. Greenlee, Electrochemical removal and recovery of phosphorus as struvite in an acidic environment using pure magnesium vs. the AZ31 magnesium alloy as the anode, Chemical Engineering Journal 380 (2020) 122480. https://doi.org/https://doi.org/10.1016/j.cej.2019.122480.

[11] L. Kékedy-Nagy, M. Abolhassani, L.F. Greenlee, B.G. Pollet, An Electrochemical Study of Ammonium Dihydrogen Phosphate on Mg and Mg Alloy Electrodes, Electrocatalysis 12 (2021) 251–263. https://doi.org/10.1007/s12678-021-00646-x.

[12] K. Govindan, S.-J. Im, V. Muthuraj, A. Jang, Electrochemical recovery of H2 and nutrients (N, P) from synthetic source separate urine water, Chemosphere 269 (2020) 129361. https://doi.org/10.1016/j.chemosphere.2020.129361.

[13] K. Rajaniemi, T. Hu, E.-T. Nurmesniemi, S. Tuomikoski, U. Lassi, Phosphate and Ammonium Removal from Water through Electrochemical and Chemical Precipitation of Struvite, Processes 9 (2021). https://doi.org/10.3390/pr9010150.
[14] S. Chandrasekaran, A. Zaffar, P. Balasubramanian, Struvite in circular economy: Production techniques, emerging applications and market opportunities, WIREs Energy and Environment 13 (2024). https://doi.org/10.1002/wene.529.
[15] V. Shrivastava, I. Laasri, Nutrient Recovery Strategies and Agronomic Performance in Circular Farming: A Comprehensive Review, Nitrogen 6 (2025) 80. https://doi.org/10.3390/nitrogen6030080.
[16] A.J. Effendi, M.S. Baashen, S. Hidayat, Nutrient Recovery From Organic-Rich Wastewater Through Struvite Precipitation using Air Cathode Electrocoagulation Technology, Air, Soil and Water Research 15 (2022) 11786221221087988. https://doi.org/10.1177/11786221221087989.
[17] I.S. Solano Huerta, G. Roa Morales, P. Balderas Hernández, C.E. Barrera Díaz, T.B. Pavón Silva, P. Ávila Pérez, I. Rodríguez Torres, Technical Considerations for Designing an Electrocoagulation Reactor for Wastewater Treatment: A Brief Review, Processes 13 (2025) 1679. https://doi.org/10.3390/pr13061679.
[18] E.R. Nuñez, G.A. Vázquez, A. Sosa, R. Nava, A. Cardenas, Alternating pulse approach for electrochemical production of struvite as an option for phosphorous recovery from wastewater, RSC Adv. 15 (2025) 28929–28936. https://doi.org/10.1039/d5ra02880a.
[19] R. Ardhianto, A. Yusrina, A.Y. Bagastyo, Iron-Based Electrocoagulation Pretreatment to Enhance Magnesium-Struvite Recovery from Livestock Wastewater Using a Tubular Reactor, Int. J. Environ. Res. 20 (2025) 41. https://doi.org/10.1007/s41742-025-00993-3.
[20] R. Ardhianto, G. Samudro, S. Mangkoedihardjo, S.T. Isratul Izmi, Integrated approach to textile wastewater treatment: Investigating electrocoagulation, MBBR, and adsorption synergy, Journal of Water Process Engineering 77 (2025) 108364. https://doi.org/https://doi.org/10.1016/j.jwpe.2025.108364.
[21] R. Ardhianto, A.D. Anggrainy, G. Samudro, A. Triyawan, A.Y. Bagastyo, A study of continuous-flow electrocoagulation process to minimize chemicals dosing in the full-scale treatment of plastic plating industry wastewater, Journal of Water Process Engineering 60 (2024) 105217. https://doi.org/https://doi.org/10.1016/j.jwpe.2024.105217.
[22] N.F. Ro'in, F.A. Dahalan, Characterization of domestic wastewater based on BOD, COD and TSS parameters, Environmental and Toxicology Management 4(2) (2024) 16–23.
[23] Y. Li, W. Wang, L. Sun, J. Cui, X. Liu, J. Liu, Y. Chang, D. Yao, A Full Chain of Applying Struvite Recovered from Biogas Slurry to Promote Vegetable Growth, Agriculture 15 (2025) 1352. https://doi.org/10.3390/agriculture15131352.
[24] M. Cherifi, S. Hazourli, S. Pontvianne, F. Lapicque, J.-P. Leclerc, Electrokinetic removal of aluminum and chromium from industrial wastewater electrocoagulation treatment sludge, Desalination Water Treat. 57 (2016) 18500–18515. https://doi.org/10.1080/19443994.2015.1094427.
[25] T.S.A. Singh, S.T. Ramesh, An experimental study of CI Reactive Blue 25 removal from aqueous solution by electrocoagulation using Aluminum sacrificial electrode: kinetics and influence of parameters on electrocoagulation performance, Desalination Water Treat. 52 (2014) 2634–2642. https://doi.org/10.1080/19443994.2013.794714.
[26] S. Yazici Guvenc, K. Dincer, G. Varank, Performance of electrocoagulation and electro-Fenton processes for treatment of nanofiltration concentrate of biologically stabilized

landfill leachate, Journal of Water Process Engineering 31 (2019) 100863. https://doi.org/https://doi.org/10.1016/j.jwpe.2019.100863.
[27] J. de-los-Ríos-Mérida, F. Guerrero, S. Arijo, M. Muñoz, I. Álvarez-Manzaneda, J. García-Márquez, B. Bautista, M. Rendón-Martos, A. Reul, Wastewater Discharge through a Stream into a Mediterranean Ramsar Wetland: Evaluation and Proposal of a Nature-Based Treatment System, Sustainability 13 (2021) 3540. https://doi.org/10.3390/su13063540.
[28] C.E. Agbangba, E. Sacla Aide, H. Honfo, R. Glèlè Kakai, On the use of post-hoc tests in environmental and biological sciences: A critical review, Heliyon 10 (2024). https://doi.org/10.1016/j.heliyon.2024.e25131.
[29] A.J.M. Salcedo, M. Cañedo-Argüelles, S.S. Kaushal, E.M. Ciriero-Cebrián, A. Perez-Blanco, H. Salvadó, Assessing the effects of salinity on microbial communities and pollutant removal in urban wastewater treatment plants, Journal of Water Process Engineering 66 (2024) 105974. https://doi.org/https://doi.org/10.1016/j.jwpe.2024.105974.
[30] G.P. Bhoi, K.S. Singh, D.A. Connor, Optimization of phosphorus recovery using electrochemical struvite precipitation and comparison with iron electrocoagulation system, Water Environment Research 95 (2023) e10847. https://doi.org/10.1002/wer.10847.
[31] E. Ariyanto, E.S. Yusmartini, Gusmiatun, Fatimah, M. Purwoko, Harnessing Electrochemical Processes for Enhanced Struvite Crystallization: A Comprehensive Review, Indonesian Journal of Fundamental and Applied Chemistry 10 (2025).
[32] L. Kékedy-Nagy, A. Teymouri, A.M. Herring, L.F. Greenlee, Electrochemical removal and recovery of phosphorus as struvite in an acidic environment using pure magnesium vs. the AZ31 magnesium alloy as the anode, Chemical Engineering Journal 380 (2020) 122480. https://doi.org/10.1016/j.cej.2019.122480.
[33] L. Wang, C. Ye, B. Gao, X. Wang, Y. Li, K. Ding, H. Li, K. Ren, S. Chen, W. Wang, X. Ye, Applying struvite as a N-fertilizer to mitigate N2O emissions in agriculture: Feasibility and mechanism, J. Environ. Manage. 330 (2023) 117143. https://doi.org/10.1016/j.jenvman.2022.117143.
[34] K. Dermentzis, D. Marmanis, A. Christoforidis, A. Moumtzakis, Photovoltaic electrocoagulation process for remediation of chromium plating wastewaters, Desalination Water Treat. 56 (2015) 1413–1418. https://doi.org/10.1080/19443994.2014.950992.
[35] R.J.N. Aka, M.M. Hossain, A. Nasir, Y. Zhan, X. Zhang, J. Zhu, Z.W. Wang, S. Wu, Enhanced nutrient recovery from anaerobically digested poultry wastewater through struvite precipitation by organic acid pre-treatment and seeding in a bubble column electrolytic reactor, Water Res. 252 (2024) 121239. https://doi.org/10.1016/j.watres.2024.121239.
[36] R. Hamdi, H. Abu Hasan, M.H. Muhamad, N.A. Nazairi, Efficient nitrogen recovery from domestic wastewater through struvite precipitation: Optimizing process parameters and characterization analysis, Ain Shams Engineering Journal 16 (2025) 103760. https://doi.org/10.1016/j.asej.2025.103760.
[37] S. Tuomikoski, E. Sauvola, M. Riponiemi, U. Lassi, J. Pesonen, Usage of phosphoric acid plant's circulate pond waters in struvite precipitation—Effect of conditions, Water and Environment Journal 37 (2023) 445–453. https://doi.org/10.1111/wej.12848.

[38] G. Santos Nunes, K.J. Sammarro Silva, B.L. Souza Freitas, V.L. Belini, L.P. Sabogal-Paz, In-situ microscopy investigation of floc development during coagulation-flocculation with chemical and natural coagulants, Sep. Sci. Technol. ahead-of-print (2022) 2312–2322. https://doi.org/10.1080/01496395.2022.2056055.
[39] A.J. Effendi, M.S. Baashen, S. Hidayat, Nutrient Recovery From Organic-Rich Wastewater Through Struvite Precipitation using Air Cathode Electrocoagulation Technology, Air, Soil and Water Research 15 (2022) 117862212210879. https://doi.org/10.1177/11786221221087989.
[40] E.I. Romadina, A. V Akkuratov, O. Simoska, K.J. Stevenson, Phenazine-Based Compound as a Universal Water-Soluble Anolyte Material for the Redox Flow Batteries, Batteries 8 (2022) 288. https://doi.org/10.3390/batteries8120288.
[41] R. Najeeb, A. Abbar, Optimization of COD Removal from Pharmaceutical Wastewater by Electrocoagulation process using Response Surface Methodology (RSM), Egypt. J. Chem. 0 (2021) 0. https://doi.org/10.21608/ejchem.2021.82809.4107.
[42] N.A. Yaranal, S.A. Kuchibhotla, S. Subbiah, K. Mohanty, Identification, removal of microplastics and surfactants from laundry wastewater using electrocoagulation method, Water Emerging Contaminants & Nanoplastics 3 (2023). https://doi.org/10.20517/wecn.2023.46.
[43] X. Li, B. Li, J. Zhao, H. Yuan, Y. Chi, Efficient Removal of Polyethylene Using Magnesium Hydroxide and Anionic Polyacrylamide as Dual-Coagulant by Coagulation-Flocculation Processes, Pol. J. Environ. Stud. (2025). https://doi.org/10.15244/pjoes/207485.
[44] R. Ardhianto, G. Samudro, S. Mangkoedihardjo, S.T.I. Izmi, Integrated approach to textile wastewater treatment: Investigating electrocoagulation, MBBR, and adsorption synergy, Journal of Water Process Engineering 77 (2025) 108364. https://doi.org/10.1016/j.jwpe.2025.108364.
[45] Y. Zhang, C. Zhao, Z. Li, D. Kong, L. Kong, pH-Self-Buffering and Flocculation-Enabled Nonradical Oxidation via Magnesium Hydroxide-Activated Peroxymonosulfate for Selective Organic Pollutant Degradation, Nanomaterials 16 (2026) 166. https://doi.org/10.3390/nano16030166.
[46] S. Fukumoto, M. Okuda, T. Matsuyama, K. Tsuji, Depth-selective x-ray diffraction using energy-dispersive x-ray detector and straight capillary optics., Rev. Sci. Instrum. 95 (2024). https://doi.org/10.1063/5.0191425.
[47] J. Greasley, P. Hosein, Exploring supervised machine learning for multi-phase identification and quantification from powder X-ray diffraction spectra, J. Mater. Sci. 58 (2023) 5334–5348. https://doi.org/10.1007/s10853-023-08343-4.
[48] C. Mazzoni, A. Piacentini, L. Di Bella, L. Aldega, C. Perinelli, A.M. Conte, M. Ingrassia, T. Ruspandini, A. Bonfanti, B. Caraba, F.G. Falese, F.L. Chiocci, S. Fazi, Carbonate precipitation and phosphate trapping by microbialite isolates from an alkaline insular lake (Bagno dell'Acqua, Pantelleria Island, Italy)., Front. Microbiol. 15 (2024) 1391968. https://doi.org/10.3389/fmicb.2024.1391968.
[49] A. Uysal, B. Yıldızbaş, Hazenite and K-struvite production: phosphorus and potassium recovery from biomass power plant bottom ash using extraction and crystallization processes, J. Mater. Cycles Waste Manag. 26 (2024) 1450–1462. https://doi.org/10.1007/s10163-024-01898-7.

[50] A. Cahil, B. Šoptrajanov, M. Najdoski, H.D. Lutz, B. Engelen, V. Stefov, Infrared and Raman spectra of magnesium ammonium phosphate hexahydrate (struvite) and its isomorphous analogues. Part VI: FT-IR spectra of isomorphously isolated species. NH4+ ions isolated in MKPO4·6H2O (M = Mg; Ni) and PO43 - ions isolated in MgNH4AsO4·6H2O, J. Mol. Struct. 876 (2008) 255–259. https://doi.org/10.1016/j.molstruc.2007.06.023.

[51] M. Al-Shannag, Z. Al-Qodah, K. Bani-Melhem, M.R. Qtaishat, M. Alkasrawi, Heavy metal ions removal from metal plating wastewater using electrocoagulation: Kinetic study and process performance, Chemical Engineering Journal 260 (2015) 749–756. https://doi.org/https://doi.org/10.1016/j.cej.2014.09.035.